PLASTIC DEFORMATION CAPACITY OF H-SHAPED STEEL BEAM CONNECTED TO CONCRETE FILLED STEEL TUBULAR COLUMN

Y. Sameshima[1], M. Kido[2] and K. Tsuda[3]

[1] *Graduate student, Graduate School of Environmental Engineering, The University of Kitakyushu, Fukuoka, Japan*
[2] *Lecturer, Dept. of Architecture, The University of Kitakyushu, Fukuoka, Japan*
[3] *Professor, Dept. of Architecture, The University of Kitakyushu, Fukuoka, Japan*
Email: kido@env.kitakyu-u.ac.jp

ABSTRACT:
The flexural strength of a beam web connected to a concrete filled circular steel tubular column is calculated by a mechanism method assuming the plastic collapse mechanisms of the column wall and the beam web. The flexural strength decreases as the diameter-thickness ratio of the column increases. The flexural strength of the beam web connected to the circular CFT column is greater than that of the beam web connected to the circular hollow steel tube. The simplified equation for calculating the flexural strength of the beam web is presented based on the analytical results. Further, the plastic deformation capacity of the beam connected to the square CFT column is calculated.

KEYWORDS:
beam-to-column connection, steel concrete composite column, plastic analysis, mechanism method

1. INTRODUCTION

Brittle fractures of welded beam end in real structures were observed in Northridge Earthquake and Hyogoken-Nanbu Earthquake. “The guideline for brittle fracture resistance at welded steel beam ends (in Japanese)” (The Building Center, 2003), which shows that the design methods for beam ends and welding procedure of beam ends, has been published for a design to prevent brittle failures. In this guideline, the evaluation formula to calculate the plastic rotation angle of an H-shaped beam connected to a square hollow section column is presented. The plastic rotation angle is an index to express the plastic deformation capacity.

The plastic deformation capacity of the beam must be large enough to absorb seismic energy. The design formula for a beam end joint is presented (AIJ, 2006).

$$ {}_jM_u = \kappa \cdot {}_bM_p \tag{1.1}$$

Where, ${}_jM_u$ is the maximum bending moment at beam ends, ${}_bM_p$ is the full plastic moment of beams and κ is a connection coefficient which is determined by the objective performance of the beam and has the value more than unity. It is necessary to consider the effect of the out-of-plane deformation of the column wall when the flexural strength of the beam web connected to the hollow section column is calculated. The flexural strength of the beam web controls plastic deformation capacity of the beam. Hence a proper estimation of strength at the beam end is required. Some formulas for flexural strengths of beam webs were proposed based on results of plastic analysis and experimental works.

In case a beam-to-column connection consists of H-shaped beams and a concrete filled steel tubular column (from now on CFT column), the out-of-plane deformation of the column wall can be prevented by infilled concrete in the part where the beam web is subjected to compressive stress. The out-of-plane deformation can be caused in the part where the beam web is subjected to tensile stress. It can be considered that the flexural

strength of the beam web connected to the CFT column also decreases due to the out-of-plane deformation. Two of authors have shown the flexural strength of the beam web connected to the square CFT column (Kido & Tsuda, 2006). However, the flexural strength of a beam web connected to the circular CFT column has not been calculated.

Objective of this paper is to calculate the flexural strength of the beam web connected to a circular CFT column and compare with the flexural strength of beam web connected to hollow steel tubes and square CFT columns. The simplified equation for calculating the beam web connected to the circular CFT column is presented. Furthermore, the deformation capacity of H-shaped steel beam connected to a square CFT column is calculated.

2. ANALYSIS OF FLEXURAL STRENGTH OF THE BEAM WEB

2.1. Assumed collapse mechanism

The collapse mechanism of the square CFT column shown by Fig.1 (a) has been proposed. The yield lines are shown by thick dotted lines. The collapse load has been calculated based on the upper bound theorem. It is assumed that the out-of-plane deformation of the column flange is prevented by infilled concrete in the area where the beam web is subjected to compressive force. And it is presumed that the deformation of the column connected to beam flanges is fixed by through-diaphragms or inner-diaphragms.

In case of a circular CFT column, the collapse mechanism is assumed as shown in Fig.1 (b). The area which has height of D_j and width of $D_m \sin\alpha$ is the column's collapse mechanism. Fig.1 (c) shows the yield area of the beam web. The beam end rotates by θ radians and moves from line p-q to line p'-q'. The part from upper and lower edges to A and B is assumed to yield in the direction of beam axis. The values of A, B and α are parameters which define the plastic collapse mechanism in the column wall.

2.2. Yield condition and internal virtual work per unit length of shallow cylindrical shells

A part of a circular steel tube is idealized as a shallow cylindrical shell. The yield condition of the shallow

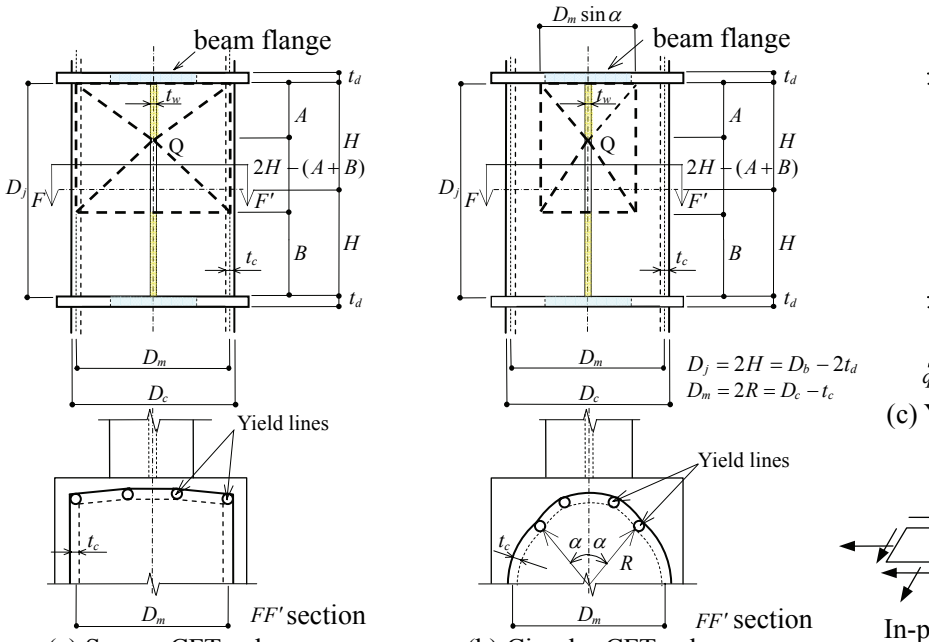

(a) Square CFT column (b) Circular CFT column

Fig. 1 Collapse mechanism of beam-column connections

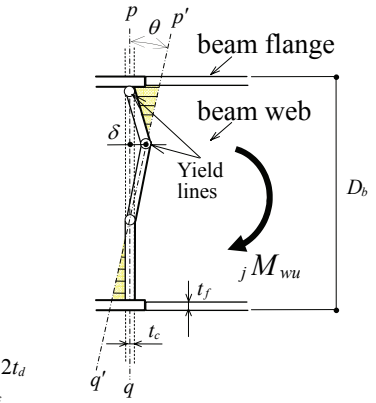

(c) Yield area at a beam web

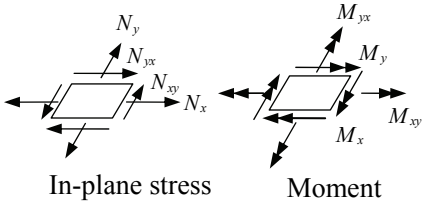

Fig. 2 Section force

cylindrical shell is idealized based on the assumptions; 1) idealized sandwich shells, 2) Mises yield condition (Yokoo et al., 1964). The yield surfaces are composed by two yield curved surfaces and the yield conditions are given by Eq. (2.1) by using the section forces shown in Fig. 2.

$$\left.\begin{aligned} F_1 &= (n_x + m_x)^2 - (n_x + m_x)(n_y + m_y) + (n_y + m_y)^2 + 3(n_{xy} + m_{xy})^2 = 1 \\ F_2 &= (n_x - m_x)^2 - (n_x - m_x)(n_y - m_y) + (n_y - m_y)^2 + 3(n_{xy} - m_{xy})^2 = 1 \end{aligned}\right\} \tag{2.1}$$

Where, $n_x = N_x / N_0$, $n_{xy} = N_{xy} / N_0$, $n_y = N_y / N_0$, $m_x = M_x / M_0$, $m_{xy} = M_{xy} / M_0$, $m_y = M_y / M_0$, $N_0 = \sigma_y t$, $M_0 = \sigma_y t^2/4$, and σ_y is yield strength and t is thickness of the shell.

Internal virtual work per unit length corresponding to discontinuous velocity fields on yield lines is given by Eq. (2.2).

$$E_i = \frac{N_0 \cdot R}{\sqrt{3}} \left\{ \sqrt{\left(\left] \tilde{u} \right] - \omega \cdot \frac{\partial w}{\partial \xi} \right] \right)^2 + \left(\frac{\left] \tilde{v} \right]}{2} \right)^2} + \sqrt{\left(\left] \tilde{u} \right] + \omega \cdot \frac{\partial w}{\partial \xi} \right] \right)^2 + \left(\frac{\left] \tilde{v} \right]}{2} \right)^2} \right\} \tag{2.2}$$

Where, $\tilde{u}$ and $\tilde{v}$ are x direction and y direction velocity components respectively in the local coordinate system on the tangent plane including one point of a yield line of the shell. w is the velocity component in the normal direction on the middle surface of the shell and $\partial w/\partial \xi$ is the velocity gradient. A symbol] denotes the discontinuous quantity crossing a yield line. The velocity components are normalized by radius R and ω is a shell parameter depending on the diameter-thickness ratio of the shell and defined by $\omega = M_0 / (N_0 R) = t/4R$.

2.3. Discontinuous quantities

The x-ϕ coordination system is defined as shown in Fig.3. The deformation velocities of generatrix, circumferential and normal direction at the middle surface of a cylindrical shell in the x-ϕ coordinate system normalized by radius R are expressed by u, v and w respectively. Normalized sizes are defined by $h = H/R$, $a = A/R$, and $b = B/R$.

The region I rotates on the A-B axis as a rigid body and the region III similarly rotates on the C-D axis. The region II rotates on the yield line (ii), the P-R axis, as a rigid body. The virtual velocity of normal direction at point Q is δ.

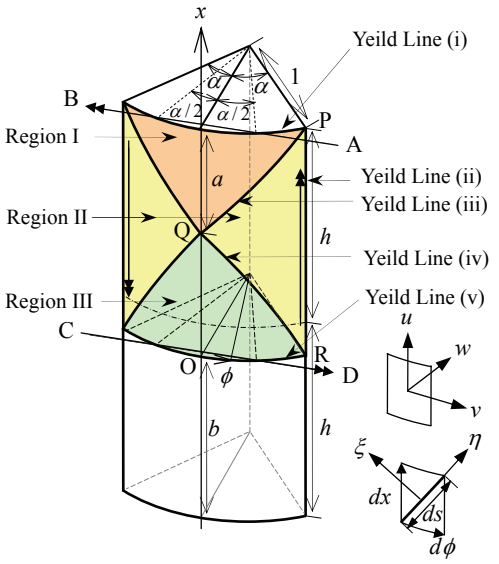

Fig. 3 Yield lines on the shell

2.3.1 Velocity component in the regions I, II and III

Velocity components in each region are shown below.

[Region I] $$u = \frac{1}{a}(\cos\phi - \cos\frac{\alpha}{2}) \cdot \delta, \quad v = -\frac{h-x}{a}\sin\phi \cdot \delta, \quad w = -\frac{h-x}{a}\cos\phi \cdot \delta \tag{2.3}$$

[Region II] $$u = 0, \quad v = \frac{\sin^2\{(\alpha-\phi)/2\}}{\sin(\alpha/2)\cdot\cos(\alpha/2)} \cdot \delta, \quad w = -\frac{\sin\{(\alpha-\phi)/2\}\cdot\cos\{(\alpha-\phi)/2\}}{\sin(\alpha/2)\cdot\cos(\alpha/2)} \cdot \delta \tag{2.4}$$

[Region III] $$u = \frac{\cos\phi - \cos(\alpha/2)}{2h-(a+b)} \cdot \delta, \quad v = -\frac{x+(b-h)}{2h-(a+b)}\sin\phi \cdot \delta, \quad w = -\frac{x+(b-h)}{2h-(a+b)}\cos\phi \cdot \delta \tag{2.5}$$

The yield lines (iii) and (iv) are given by Eqs. (2.6) and (2.7) depending on the continuous condition that the deformation velocities of normal direction *w* must be continuous.

Yield line (iii)
$$h-x=\frac{a}{\cos\phi}\cdot\frac{\sin\{(\alpha-\phi)/2\}\cdot\cos\{(\alpha-\phi)/2\}}{\sin(\alpha/2)\cdot\cos(\alpha/2)} \tag{2.6}$$

Yield line (iv)
$$x+(b-h)=\frac{2h-(a+b)}{\cos\phi}\cdot\frac{\sin\{(\alpha-\phi)/2\}\cdot\cos\{(\alpha-\phi)/2\}}{\sin(\alpha/2)\cdot\cos(\alpha/2)} \tag{2.7}$$

2.3.2 Discontinuous quantity

[Yield line (i)]
$$\tilde{u}\rceil=-\frac{1}{a}(\cos\phi-\cos\frac{\alpha}{2})\cdot\delta,\quad \tilde{v}\rceil=0,\quad \left\lceil\frac{\partial w}{\partial\xi}\right\rceil=\frac{1}{a}\cos\phi\cdot\delta \tag{2.8}$$

[Yield line (ii)]
$$\tilde{u}\rceil=0,\quad \tilde{v}\rceil=0,\quad \left\lceil\frac{\partial w}{\partial\xi}\right\rceil=\frac{1}{2\sin(\alpha/2)\cdot\cos(\alpha/2)}\cdot\delta \tag{2.9}$$

[Yield line (iii)]
$$\left.\begin{aligned}
\tilde{u}\rceil&=\frac{1}{a}(\cos\phi-\cos\frac{\alpha}{2})\frac{d\phi}{ds}\cdot\delta+\frac{\sin(\frac{\alpha-\phi}{2})\cdot\cos(\frac{\alpha-\phi}{2})\cdot\tan\phi+\sin^2(\frac{\alpha-\phi}{2})}{\sin(\alpha/2)\cdot\cos(\alpha/2)}\cdot\frac{dx}{ds}\cdot\delta\\
\tilde{v}\rceil&=\frac{1}{a}(\cos\phi-\cos\frac{\alpha}{2})\frac{dx}{ds}\cdot\delta-\frac{\sin(\frac{\alpha-\phi}{2})\cdot\cos(\frac{\alpha-\phi}{2})\cdot\tan\phi+\sin^2(\frac{\alpha-\phi}{2})}{\sin(\alpha/2)\cdot\cos(\alpha/2)}\cdot\frac{d\phi}{ds}\cdot\delta\\
\left\lceil\frac{\partial w}{\partial\xi}\right\rceil&=-\frac{1}{a}\cos\phi\cdot\frac{d\phi}{ds}\cdot\delta+\frac{1}{\sin(\alpha/2)\cos(\alpha/2)}\times\left\{\sin\left(\frac{\alpha-\phi}{2}\right)\cos\left(\frac{\alpha-\phi}{2}\right)\tan\phi+\frac{1}{2}\sin^2\left(\frac{\alpha-\phi}{2}\right)-\frac{1}{2}\cos^2\left(\frac{\alpha-\phi}{2}\right)\right\}\cdot\frac{dx}{ds}\cdot\delta
\end{aligned}\right\} \tag{2.10}$$

[Yield line (iv)]
$$\left.\begin{aligned}
\tilde{u}\rceil&=-\frac{1}{2h-(a+b)}(\cos\phi-\cos\frac{\alpha}{2})\frac{d\phi}{ds}\cdot\delta-\frac{\sin(\frac{\alpha-\phi}{2})\cdot\cos(\frac{\alpha-\phi}{2})\cdot\tan\phi+\sin^2(\frac{\alpha-\phi}{2})}{\sin(\alpha/2)\cdot\cos(\alpha/2)}\cdot\frac{dx}{ds}\cdot\delta\\
\tilde{v}\rceil&=-\frac{1}{2h-(a+b)}(\cos\phi-\cos\frac{\alpha}{2})\frac{dx}{ds}\cdot\delta+\frac{\sin(\frac{\alpha-\phi}{2})\cdot\cos(\frac{\alpha-\phi}{2})\cdot\tan\phi+\sin^2(\frac{\alpha-\phi}{2})}{\sin(\alpha/2)\cdot\cos(\alpha/2)}\cdot\frac{d\phi}{ds}\cdot\delta\\
\left\lceil\frac{\partial w}{\partial\xi}\right\rceil&=-\frac{1}{2h-(a+b)}\cos\phi\cdot\frac{d\phi}{ds}\cdot\delta-\frac{1}{\sin(\alpha/2)\cos(\alpha/2)}\times\left\{\sin\left(\frac{\alpha-\phi}{2}\right)\cos\left(\frac{\alpha-\phi}{2}\right)\tan\phi+\frac{1}{2}\sin^2\left(\frac{\alpha-\phi}{2}\right)-\frac{1}{2}\cos^2\left(\frac{\alpha-\phi}{2}\right)\right\}\cdot\frac{dx}{ds}\cdot\delta
\end{aligned}\right\} \tag{2.11}$$

[Yield line (v)]
$$\tilde{u}\rceil=\frac{\cos\phi-\cos(\alpha/2)}{2h-(a+b)}\cdot\delta,\quad \tilde{v}\rceil=0,\quad \left\lceil\frac{\partial w}{\partial\xi}\right\rceil=\frac{1}{2h-(a+b)}\cos\phi\cdot\delta \tag{2.12}$$

Where, *ds* is the infinitesimal length of yield lines (See also Fig.3).

2.4 Internal virtual work and collapse load

Equations (2.8) ~ (2.12) are substituted into Eq. (2.2) and integrating Eq. (2.2) along yield lines gives internal virtual work of each yield line.

$$\left.\begin{aligned} E_{(\mathrm{i})} &= \frac{2_c N_y \cdot R^2}{\sqrt{3}}\left(\int_0^{\alpha}\left|\tilde{u}\right]+\omega\frac{\partial w}{\partial \xi}\right]\right|+\left|\tilde{u}\right]-\omega\frac{\partial w}{\partial \xi}\right]\right| d\phi\Big), \qquad E_{(\mathrm{ii})} = \frac{4_c N_y \cdot R^2}{\sqrt{3}} h\left|\omega\frac{\partial w}{\partial \xi}\right] \right| \\ E_{(\mathrm{iii})} &= \int_{\mathrm{QP}} E_i ds, \qquad E_{(\mathrm{iv})} = \int_{\mathrm{QR}} E_i ds, \qquad E_{(\mathrm{v})} = \frac{2_c N_y \cdot R^2}{\sqrt{3}}\left(\int_0^{\alpha}\left|\tilde{u}\right]+\omega\frac{\partial w}{\partial \xi}\right]\right|+\left|\tilde{u}\right]-\omega\frac{\partial w}{\partial \xi}\right]\right| d\phi\Big) \end{aligned}\right\} \tag{2.13}$$

Where, ${}_cN_y={}_c\sigma_y\, t_c$ (${}_c\sigma_y$: yield strength of a steel tube)
From Eq. (2.13), total internal virtual work of the circular CFT column wall is given by Eq. (2.14).

$$E_c = E_{(\mathrm{i})} + E_{(\mathrm{ii})} + E_{(\mathrm{iii})} + E_{(\mathrm{iv})} + E_{(\mathrm{v})} \tag{2.14}$$

The internal virtual work of the beam web is given by Eq. (2.15).

$$E_b = {}_bN_y \cdot R^2 \cdot \frac{a(2h-b)+b^2}{4h-2(a+b)} \cdot \delta \tag{2.15}$$

Where, ${}_bN_y={}_b\sigma_y\, t_w$ (${}_b\sigma_y$: yield strength of a beam web). The upper bound collapse load of the beam web joints ${}_jM_{wu}$ is calculated by equating the external virtual work with the internal virtual work.

$${}_jM_{wu} \cdot \frac{\delta}{2h-(a+b)} = E_c + E_b \tag{2.16}$$

The most proper upper bound is obtained by Eq. (2.17)

$$\frac{\partial\, {}_jM_{wu}}{\partial \alpha} = 0, \quad \frac{\partial\, {}_jM_{wu}}{\partial a} = 0, \quad \frac{\partial\, {}_jM_{wu}}{\partial b} = 0 \tag{2.17}$$

3. EXAMPLES OF ANALYSIS AND NONDIMENSIONAL FLEXURAL STRENGTH

A closed form solution can not be obtained by Eq. (2.16) and the nondimensional flexural strength m_c is calculated by numerical integration. The flexural strength m_c is defined by Eq. (3.1).

$$m_c = {}_jM_{wu} / M_{wp} \tag{3.1}$$

Where, M_{wp} is a full plastic moment of the beam web $M_{wp}=h^2 \cdot R^2 \cdot {}_bN_y$. The upper limit of the flexural strength m_c is unity. The analysis is carried out by setting $\beta = {}_bN_y/{}_cN_y$ as given by Eq. (3.2) and ${}_b\sigma_y={}_c\sigma_y$ and $D_j/t_w=40$.

$$\beta = \frac{{}_bN_y}{{}_cN_y} = \frac{{}_b\sigma_y \cdot t_w}{{}_c\sigma_y \cdot t_c} = \frac{{}_b\sigma_y}{{}_c\sigma_y} \cdot \frac{t_w}{D_j} \cdot \frac{D_m}{t_c} \cdot h \tag{3.2}$$

3.1 comparisons with the hollow circular steel tube and the square CFT column

Figure 4 shows the relation between the flexural strength and the diameter thickness ratio. The flexural strengths of the beam web in case of the circular CFT column are shown by thick solid lines and the flexural strengths of beam web in case of the hollow circular tube are shown by thin solid lines. The flexural strength in case of hollow circular tubes was calculated by the method which has been already proposed (Tanaka, et al., 2001). The aspect ratio h varies 1, 1.5 and 2. According to Fig.4, the flexural strength in case of the CFT columns is greater than that in case of the hollow tube when the diameter thickness ratio and the aspect ratio are same. The flexural

strength decreases as the aspect ratio increases.
Figure 5 shows the flexural strength of the beam web in case of the circular CFT column (m_c) and the square CFT column (m_0). The flexural strength in case of the circular CFT and the square CFT column are shown by thick solid lines and thin solid lines respectively. When the diameter-thickness ratio and the aspect ratio are same, the flexural strength in case of the circular column is greater than that in case of the square column.

3.2 collapse mode

Figure 6 shows the relation between the width of the collapse mechanism (the angle α) and the diameter-thickness ratio. The limit diameter-thickness ratios in case of m_c=1 are shown by white circles. According to the figure, the angle does not depend on the aspect ratio and decreases as the diameter-thickness ratio increases. When the diameter-thickness ratio is above 20, a range of angle α is $\alpha \le 0.31$rad ($\le 18°$) and the collapse mechanism is formed in shallow area of the shell.

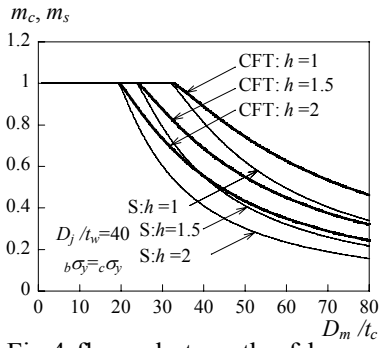

Fig.4 flexural strength of beam web in case of CFT columns and hollow columns

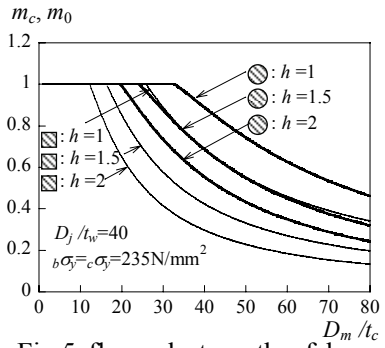

Fig.5 flexural strength of beam web in case of circular and square CFT columns

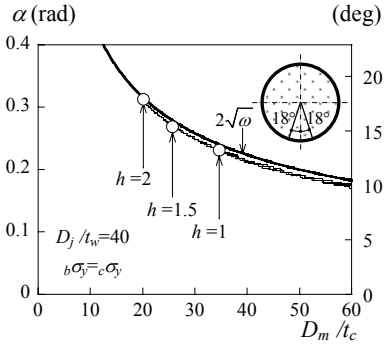

Fig.6 width of collapse mechanism

4. SIMPLEIFID EQUATION FOR THE Flexural STRENGTH OF THE BEAM WEB

4.1 Approximation and estimate equation

In this chapter, the simplified equation to calculate the flexural strength is proposed. The collapse mechanism is formed in the shallow area of the shell. Consequently internal virtual work can be approximated by focusing on the velocity gradients on yield lines and neglecting terms $\tilde{u}]$ and $\tilde{v}]$ in Eq. (2.2). The velocity component in normal direction w is approximated by Eq. (4.1).

$$w \cong -\left(1-\frac{\sin\phi}{\sin\alpha}\right)\cdot\delta \tag{4.1}$$

Equations (2.6) and (2.7) are simplified by substituting Eq. (4.1) into them. The total internal virtual work of the column wall can be approximated by using the approximation $\sin\alpha \cong \alpha$ and $\cos\alpha \cong 1$.

$$E_c \cong \frac{4}{\sqrt{3}}{}_cN_y\cdot R^2\cdot\omega\cdot\left\{\frac{2\alpha}{a}+\frac{2\alpha}{2h-(a+b)}+\frac{2(2h-b)}{\alpha}\right\}\cdot\delta \tag{4.2}$$

The collapse load is obtained by Eq. (4.3)

$$m_c \cong \frac{a(2h-b)+b^2}{2h^2}+\frac{4\omega}{\sqrt{3}\beta}\left\{\frac{4\alpha}{ah}-\frac{2b\alpha}{ah^2}+\frac{8}{\alpha}-\frac{4(a+2b)}{\alpha h}+\frac{2b(a+b)}{\alpha h^2}\right\} \tag{4.3}$$

The width of collapse mechanism depends on the diameter-thickness ratio. The angle α can be approximated by equation $\alpha \cong 2\sqrt{\omega}$. In Fig. 6, the approximated curve is shown. Substituting $\alpha \cong 2\sqrt{\omega}$ into Eq. (4.3) gives simplified equation of the collapse load Eq. (4.4).

$$m_c \cong \frac{a(2h-b)+b^2}{2h^2} + \frac{4\omega}{\sqrt{3}\beta h}\left\{\frac{4\sqrt{\omega}(2h-b)}{ah} + \frac{2(2h-a-2b)}{\sqrt{\omega}} + \frac{b(a+b)}{h\sqrt{\omega}}\right\} \tag{4.4}$$

However, a and b in Eq. (4.4) are obtained by $\partial_j M_{wu}/\partial a = 0$, $\partial_j M_{wu}/\partial b = 0$ and given by Eq. (4.5).

$$a = \frac{4\sqrt{\omega}}{\sqrt{\sqrt{3}\beta/2\sqrt{\omega}-4}}, \qquad b = \frac{32\sqrt{\omega}(\omega+ah) - a^2\left(8\sqrt{\omega}-\sqrt{3}\beta\right)}{2a\left(8\sqrt{\omega}+\sqrt{3}\beta\right)} \tag{4.5}$$

4.2 Flexural strength obtained by the simplified equation

Figure7 shows the relation between the flexural strength and the diameter-thickness ratio. The flexural strength obtained by plastic analysis in chapter 3 and simplified equation Eq.(4.4) are shown in thick solid lines (accurate value) and thin solid lines (estimated value) respectively. The flexural strength obtained by simplified equation is about 10% less than the flexural strength obtained by plastic analysis. Therefore Eq. (4.4) is applicable for calculating the flexural strength of the beam web connected to a circular CFT column.

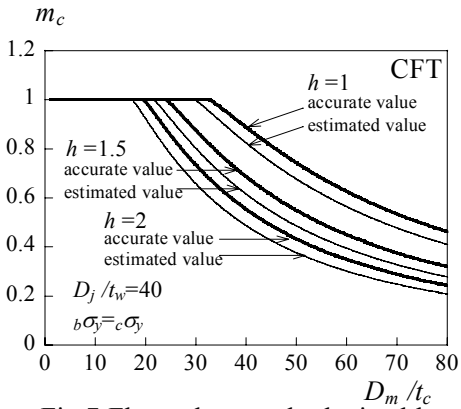

Fig.7 Flexural strength obtained by simplified equation

5. PLASTIC DEFORMATION CAPACITY OF BEAMS CONNECTED TO A CFT COLUMN

5.1 Calculation of maximum plastic rotation angle

The formula to calculate the maximum plastic rotation angle of the cantilever beam has been presented (The Building Center, 2001). The maximum plastic rotation angle expresses the plastic deformation capacity of the beam. In this paper the formula is applied to the beam connected to a square CFT column although this formula has been used for the H shaped beam connected to the square hollow column. The ineffective parts of the beam are defined by the triangle area as shown in Fig. 8. The maximum plastic rotation angle of the beam shown in Fig8 is calculated by Eq. (5.1).

$$_a\theta_{bpm} = \frac{F_{wy}}{E}\cdot\frac{L}{D_b}\cdot\frac{j\cdot(\kappa-1)}{(k+1)\cdot(k+2)\cdot(\kappa_0-1)^2\cdot\kappa^2}\times\left\{\kappa_0^{b+1}\cdot\left[(k+1)\cdot(\kappa_0-1)\cdot\kappa+(\kappa_0-\kappa)\right]-\left[k\cdot(\kappa_0-1)+(\kappa_0-\kappa)\right]\right\} \tag{5.1}$$

Where, L is the length of the beam, E is Young's modulus, j and k are coefficients defined by the strength of the beam flange and the yield ratio YR. Notations κ_0 and κ are the connection coefficients in case that the web is fully effective and partially effective and given by Eqs.(5.2) and (5.3) respectively.

$$\kappa_0 = \frac{_jM_{u0}}{_bM_p} = \frac{\gamma_f}{YR}\cdot\frac{_fZ_p}{Z_p} + \left(1-\frac{_fZ_p}{Z_p}\right) \tag{5.2}$$

$$\kappa = \frac{_jM_u}{_bM_p} = \frac{_jM_u}{Z_p\cdot F_{wy}} \tag{5.3}$$

Where, $_bM_p$ is a plastic moment of the beam, γ_f is the joint fracture strength coefficient, $_fZ_p$ and Z_p are the plastic section modulus of the beam flange and the beam section respectively. $_jM_{u0}$ and $_jM_u$ are the maximum strengths of the beam end when the beam web is all effective or the beam web is not all effective. These maximum

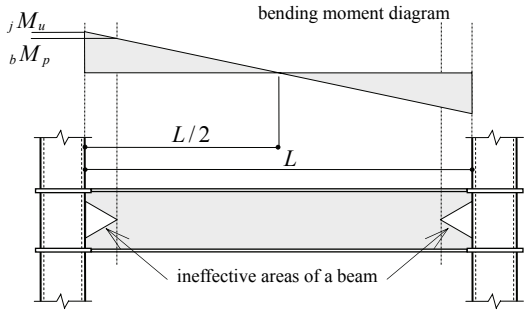

Fig.8 Analysis model

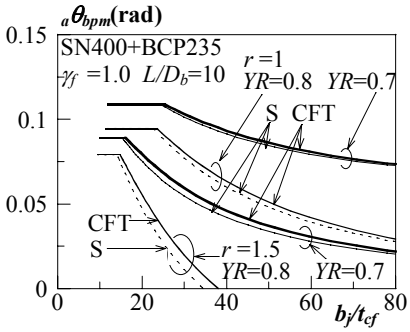

Fig.9 The maximum rotation angle

strengths are evaluated by sum of the beam flange strength and the beam web strength. The flexural strength of the beam considering the out-of-plane deformation is used in this calculation. The flexural strength of the beam connected the square CFT column that we have proposed and the flexural strength of the beam connected to a square bare tube (Suita & Tanaka, 2000) are used.

5.2 The maximum plastic rotation angle of beams connected to hollow columns and CFT columns

Example calculations are presented. The calculation is carried out by using conditions as follows; 1) the joint fracture strength coefficient γ_f is 1.0, 2) L/D_b=10, 3) material of the beam is SN400 and the column is BCP 235, 4) the yield ratio *YR* are 0.70 and 0.80 and 5) the aspect ratio $r = D_j / D_m$ are 1.0 and 1.5. Fig. 9 shows the relation between maximum plastic rotation angle and width-thickness ratio. The plastic rotation angle in case of the CFT column is greater than that in case of the hollow steel tube. The plastic rotation angle decrease as the yield ratio *YR* and the aspect ratio *r* increase.

6. CONCLUSIONS

The flexural strength of a beam web connected to a circular CFT column is calculated by a mechanism method. The plastic deformation capacity of the beam connected to square CFT is calculated. Conclusions can be drawn as follows:

1) The flexural strength of the beam web connected to the concrete filled circular steel tubular column is greater than that of the beam web connected to the hollow circular column.
2) The simplified equation Eq. (4.4) is applicable for calculating the flexural strength of the beam web connected to the concrete filled circular steel tubular column.
3) The maximum plastic rotation angle of the beams connected to the square CFT column is presented.

REFERENCES

The Building Center of Japan (2003), The guideline for brittle fracture resistance at welded steel beam ends, 2nd Edition (in Japanese)

Architectural Institute of Japan (AIJ) (2006), Recommendation for Design of Connections in Steel Structures, 1st edition, (in Japanese).

Tanaka, T., Tabuchi, M. and Murakami, H. (2001), *Flexural strength of H-beam web connected with circular hollow section columns, Journal of Constructional Steel*, **Vol.9**, pp.457-464, (in Japanese)

Kido, M., Tsuda, K. (2006), *Flexural strength of beam web to concrete filled square steel tubular column joints*, Proc. of the 8th international conference on Steel, Space & Composite Structures, pp.435-441

Yokoo, Y., Nakamura, Y. and Matsui, T. (1964), *Limit analysis of shallow parabolic cylindrical shells*, Transaction of AIJ, **No. 106**, pp.10-19

Suita, K. and Tanaka, T. (2000), Flexural strength of beam web to square tube column joints, Steel construction engineering, **Vol.7, No.26**, pp.51-58 (in Japanese).